

Gas-Phase Reactivity of Protonated 2-, 3-, and 4-Dehydropyridine Radicals Toward Organic Reagents

Anthony Adeuya,[†] Jason M. Price,[‡] Bartłomiej J. Jankiewicz, John J. Nash, and Hilikka I. Kenttämäa*

Department of Chemistry, Purdue University, West Lafayette, Indiana 47907

Received: February 15, 2009; Revised Manuscript Received: September 17, 2009

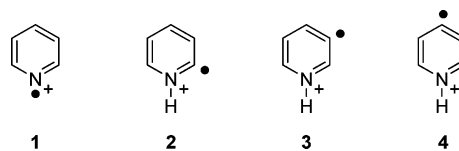
To explore the effects of the electronic nature of charged phenyl radicals on their reactivity, reactions of the three distonic isomers of *n*-dehydropyridinium cation ($n = 2, 3, \text{ or } 4$) have been investigated in the gas phase by using Fourier-transform ion cyclotron resonance mass spectrometry. All three isomers react with cyclohexane, methanol, ethanol, and 1-pentanol exclusively via hydrogen atom abstraction and with allyl iodide mainly via iodine atom abstraction, with a reaction efficiency ordering of $2 > 3 > 4$. The observed reactivity ordering correlates well with the calculated vertical electron affinities of the charged radicals (i.e., the higher the vertical electron affinity, the faster the reaction). Charged radicals **2** and **3** also react with tetrahydrofuran exclusively via hydrogen atom abstraction, but the reaction of **4** with tetrahydrofuran yields products arising from nonradical reactivity. The unusual reactivity of **4** is likely to result from the contribution of an ionized carbene-type resonance structure that facilitates nucleophilic addition to the most electrophilic carbon atom (C-4) in this charged radical. The influence of such a resonance structure on the reactivity of **2** is not obvious, and this may be due to stabilizing hydrogen-bonding interactions in the transition states for this molecule. Charged radicals **2** and **3** abstract a hydrogen atom from the substituent in both phenol and toluene, but **4** abstracts a hydrogen atom from the phenyl ring, a reaction that is unprecedented for phenyl radicals. Charged radical **4** reacts with *tert*-butyl isocyanide mainly by hydrogen cyanide (HCN) abstraction, whereas CN abstraction is the principal reaction for **2** and **3**. The different reactivity observed for **4** (as compared to **2** and **3**) is likely to result from different charge and spin distributions of the reaction intermediates for these charged radicals.

Introduction

The mechanisms of hydrogen atom abstraction by radicals have been of interest for decades.¹ However, the ability to predict the rates of such seemingly “simple” reactions has proven to be a challenge due to a poor understanding of the nature of the transition states for these reactions. As a result, the factors that control the efficiency of hydrogen atom abstraction for different types of radicals are still not well-understood. However, such knowledge could be extremely valuable, for example, for a better understanding of radical-induced DNA degeneration and the design of less cytotoxic pharmaceuticals.^{2–10} Several studies have suggested that the biological activity of some potent antitumor antibiotics arises from the formation of aromatic carbon-centered σ,σ -biradical^{11–13} intermediates that can abstract hydrogen atoms from the sugar moiety in DNA.^{12,14,15} These intermediates are so reactive that they result in high cytotoxicity.⁷ Therefore, improving the understanding of the reactivity of mono- and biradicals (particularly phenyl radicals) has become an area of intense research.^{16–18} A better understanding of the parameters that control these reactions could aid in the development of less toxic drugs.

One of the challenges faced in the examination of the reactivity of these highly reactive intermediates is their short lifetime in solution.^{12,15} Gas-phase studies provide a solvent-

free environment that eliminates competing reactions with reagents other than those of interest. Fourier-transform ion cyclotron resonance mass spectrometry (FT-ICR) has been employed in the examination of the reactivity of a variety of radicals toward neutral reagents.¹⁸ These gas-phase studies utilize the “distonic ion” approach that involves studying reactive radicals via their derivatives that carry an inert charged group for manipulation in the FT-ICR mass spectrometer.¹⁸ This study was inspired by the need to better understand the influence of charge on the reactivity of charged phenyl radicals. Here, the first direct comparison of the chemical properties of the three distonic isomers of the pyridine radical cation is reported with the goal of exploring the effects of different radical/formal charge site distances on the reactivity of charged phenyl radicals.



The 2-, 3-, and 4-dehydropyridinium cations (**2–4**) were chosen for this study because they are known¹⁹ to be stable toward isomerization by 1,2-hydrogen atom shifts to pyridine radical cation (**1**) in the gas phase. Charged radicals **2–4** differ in not only the distance between the radical and formal charge sites but also electrophilicity. Previous studies¹⁸ have suggested that as the electrophilicity of a charged phenyl radical increases, the transition states for its reactions become more polar, and

* E-mail: hilikka@purdue.edu.

[†] Current address: Arkansas Regional Lab, U.S. Food and Drug Administration, 3900 NCTR Road, Jefferson, AR 72079.

[‡] Current address: Procter and Gamble Company, Sharon Woods Technical Center, 11511 Reed Hartman Hwy., Cincinnati, OH 45241.

consequently, the transition state energy is lowered. Further, the relative electrophilicities of charged phenyl radicals can be estimated by using their (calculated) vertical electron affinities (EA_v ; defined as the energy released when an electron is added to the radical site). The results reported here shed some light on the importance of polar effects on the reactivity of isomeric charged phenyl radicals.

Experimental Methods

All experiments were carried out by using a Finnigan FTMS 2001 FT-ICR with an Odyssey data station. This instrument contains a dual cell consisting of two identical 2 in. cells collinearly aligned with the magnetic field produced by a 3 T superconducting magnet. The two cells are separated by a common wall called the “conductance limit” that contains a 2 mm hole in the center for transfer of ions between the two cells. This plate and the other trapping plates were maintained at +2 V unless specified otherwise. The two cells are differentially pumped by two Edward diffusion pumps (800 L/s), and each is backed by an Alcatel 2012 mechanical pump. A nominal base pressure of less than 1×10^{-9} Torr was indicated by an ionization gauge on each side of the dual cell.

All reagents and the precursors to the ions (2-, 3-, and 4-iodopyridine) were commercially available and were used as received. Methanol was introduced into one of the two reaction cells of the instrument via a batch inlet system equipped with an Andonian variable leak valve. Electron ionization (EI: typically 15–30 eV electron energy, 50–80 ms ionization time, and 5–10 μ A filament current) of methanol yields the molecular ion and fragment ions that react with methanol to yield protonated methanol. The charged radical precursors (introduced through a Varian leak valve into the cell containing protonated methanol) were allowed to react for ~ 3 s with protonated methanol to yield the 2-, 3-, and 4-iodopyridinium cations. The 2-, 3-, and 4-iodopyridinium cations were transferred into the second cell by grounding the conductance limit plate for ~ 144 μ s and cooled for about 1 s (i.e., by emission of light and collisions with the neutral molecules present in the cell). The technique of sustained off-resonance irradiated collision-activated dissociation²⁰ with argon target gas (introduced into the cell via a pulsed valve assembly at 1×10^{-5} Torr peak nominal pressure) was used to homolytically cleave the carbon–iodine bond. This was performed by continuously exciting the ions for 1 s at a frequency 1 kHz higher than the cyclotron frequency of the ions. The desired charged radical was isolated by ejecting all other ions via a series of stored-waveform inverse Fourier transform excitation pulses applied to the plates of the cell.²¹ All neutral reagents, with the exception of phenol (introduced through a Varian leak valve), were introduced through batch inlet systems equipped with an Andonian variable leak valve. The isolated charged radicals of interest were allowed to react with a desired neutral reagent (at a nominal pressure of 1.0×10^{-8} – 1.2×10^{-7} Torr) for a variable period of time (typically 0.05–100 s). Ion excitation for detection was achieved using a “chirp” of a bandwidth of 2.56 MHz and a sweep rate of 3200 Hz/ μ s. Each spectrum was collected as 64k data points with one zero fill prior to Fourier transformation. All measured reaction spectra were background-corrected as reported previously.¹⁸ A background spectrum was collected in the absence of the isolated ion of interest. The spectrum was subtracted from the reaction spectrum to remove peaks that are not due to the isolated ion’s reaction products.

All reactions studied under the conditions described above follow pseudo-first-order kinetics, which allows for the deriva-

tion of the second-order reaction rate constant (k_{exp}) from a semilogarithmic plot of the relative abundance of the reactant ion versus reaction time. The precision of the measured rate constants is better than $\pm 10\%$, and the absolute accuracy is estimated to be $\pm 50\%$. The theoretical collision rate constants (k_{coll}) were obtained by using a parameterized trajectory theory.²² The efficiency of each reaction (i.e., the fraction of collisions that leads to reaction) is given by $k_{\text{exp}}/k_{\text{coll}}$. The greatest error arises from the cell pressure measurement. The pressure readings of the ion gauges were corrected for their sensitivity toward each neutral reagent.²³ This correction was obtained by measuring the reaction efficiency of highly exothermic proton transfer from protonated acetone and electron transfer to carbon disulfide radical cation for the reagent of interest. These reactions are assumed to occur at collision rate. Primary reaction products were identified on the basis of the constant ratio of their relative abundances at short reaction times. The product branching ratios were determined by dividing the abundance of each primary product ion by the sum of all primary product ion abundances.

Computational Methods

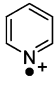
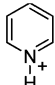
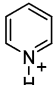
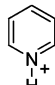
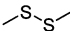
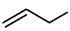
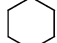
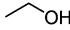
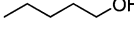
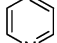
Electronic energies and thermally corrected (298 K) enthalpies for all ground-state species and transition states were computed at the G3MP2B3 level of theory.²⁴ In the G3MP2B3 procedure, molecular geometries are optimized at the density functional (DFT) level of theory by using the 6-31G(d) basis set.²⁵ These DFT calculations use the three-parameter exchange functional of Becke,²⁶ which is combined with the gradient-corrected correlation functional of Lee, Yang, and Parr²⁷ (B3LYP). All DFT geometries were verified to be local minima by computation of analytic vibrational frequencies. DFT calculations for doublet states employed an unrestricted formalism, and total spin expectation values for Slater determinants formed from the optimized Kohn–Sham orbitals did not exceed 0.77.

To compute EA_v for the three charged aryl radicals, the geometries were optimized at the B3LYP level of theory by using the correlation-consistent polarized valence-triple- ζ (cc-pVTZ²⁸) basis set. Single-point calculations (B3LYP/aug-cc-pVTZ²⁸) using the optimized geometry for each charged aryl radical were also carried out for the states that are produced when a single electron is added to the nonbonding σ orbital of each molecule.²⁹ For the charged aryl radicals studied here, these calculations involve (zwitterionic) singlet states.³⁰ The vertical electron affinities of the charged aryl radicals were computed as $[E_0(\text{monoradical}; \text{doublet state})] - [E_0(\text{monoradical} + \text{electron}; \text{singlet state})]$. Note that because these are vertical electron affinities, zero-point vibrational energies (ZPVEs) and 298 K thermal contributions to the enthalpy are not included.

Atomic charges were calculated at the B3LYP/cc-pVDZ²⁸ level of theory by using the B3LYP/6-31G(d) optimized geometries (e.g., obtained from the G3MP2B3 calculations) and the CHELPG procedure.³¹ For these calculations, the atomic charges were fitted to reproduce the overall molecular dipole moment.

Molecular geometries for the three charged aryl radicals, methanol, ethanol, and tetrahydrofuran as well as the hydrogen-atom abstraction transition states for each of the charged aryl radicals with methanol, ethanol, and tetrahydrofuran were also optimized at the MPW1K level of theory^{32,33} by using the 6-31+G(d,p) basis set.^{25,34} The MPW1K functional is a modification of the Perdew–Wang gradient-corrected exchange functional, with one parameter optimized to give the best fit to kinetic data for forty radical reactions.³² All MPW1K geometries were verified to be local minima (or transition states) by

TABLE 1: Reaction Efficiencies^a (Eff.) and Primary Product Branching Ratios for Reactions of Charged Radicals 1–4 with Dimethyl Disulfide, Allyl Iodide, Cyclohexane, Methanol, Ethanol, 1-Pentanol, and Pyridine

	 1	 2	 3	 4
	electron abs 96% H abs 4% Eff. = 99%	CH ₃ S abs 94% H abs 5% SSCH ₃ abs 1% Eff. = 79%	CH ₃ S abs 100% Eff. = 77%	CH ₃ S abs 100% Eff. = 75%
	not studied	I abs 84% allyl abs 16% Eff. = 69%	I abs 90% allyl abs 10% Eff. = 57%	I abs 92% allyl abs 8% Eff. = 53%
	not studied	H abs 100% Eff. = 33%	H abs 100% Eff. = 17%	H abs 100% Eff. = 13%
CH ₃ OH	not studied	H abs 100% Eff. = 21%	H abs 100% Eff. = 1.7%	H abs 100% Eff. = 0.4%
	not studied	H abs 100% Eff. = 33%	H abs 100% Eff. = 11%	H abs 100% Eff. = 4.2%
	not studied	H abs 100% Eff. = 88%	H abs 100% Eff. = 53%	H abs 100% Eff. = 43%
	not studied	H ⁺ transfer 100% Eff. = 52%	H ⁺ transfer 100% Eff. = 51%	H ⁺ transfer 100% Eff. = 46%

^a Reaction efficiencies are reported as $k_{\text{exp}}/k_{\text{coll}} \times 100\%$.

computation of analytic vibrational frequencies, and these (unscaled) frequencies were used to compute ZPVEs and 298 K thermal contributions ($H_{298} - E_0$) for all species. “Activation enthalpies” for the three charged aryl radicals were computed as the difference in enthalpy between the transition state and the separated reactants (i.e., charged aryl radical and either methanol, ethanol or tetrahydrofuran). MPW1K calculations for the three charged aryl radicals and the transition states employed an unrestricted formalism.

All G3MP2B3 and DFT calculations were carried out with the Gaussian 03³⁵ electronic structure program suite.

Results

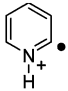
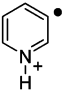
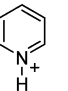

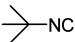
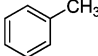
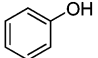
Gas-phase reactions of the isolated charged radicals **2–4** were examined with dimethyl disulfide, allyl iodide, cyclohexane, methanol, ethanol, 1-pentanol, pyridine, tetrahydrofuran, *tert*-butyl isocyanide, toluene, and phenol. Reaction efficiencies and product branching ratios are listed in Tables 1 and 2. Predominant thiomethyl (CH₃S) abstraction from dimethyl disulfide by all three charged radicals (Table 1) provides strong evidence for the expected^{36a} distonic ion structures (the conventional pyridine radical cation (**1**) has a higher electron affinity (EA = 9.25 eV)^{37a} than most distonic ions and reacts with dimethyl disulfide (IE = 8.2 eV)^{37b} mainly by (exothermic) electron

abstraction). Moreover, differentiation of **2–4** is possible due to the large differences in their reaction efficiencies (e.g., 33%, 11%, and 4.2% with ethanol, and 21%, 1.7%, and 0.4% with methanol, respectively; Table 1). In all experiments, the decay in the reactant ion population follows pseudo-first-order kinetics, which indicates that the ion populations are isomerically pure (typically, ~2% of an unreactive isomer must be present to observe deviation from pseudo first-order kinetics).

Discussion

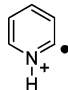
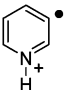
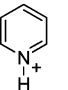
Although a detailed analysis of the relative reaction rates is beyond the scope of this work, the reaction rates may provide insight to the reaction mechanisms for charged radicals **2–4** with the various neutral reagents. Hence, several previous studies on the parameters that control the relative reaction rates of charged phenyl radicals are pertinent to this work. For example, it has been demonstrated that the reaction rates for charged phenyl radicals depend only on the energy of the transition state (more specifically, the difference in energy between the separated reactants and the transition state).³⁸ Furthermore, observations for a series of charged phenyl radicals that exhibit identical reactivity toward several neutral reagents, despite differences in the magnitude of the dipole moment, dipole orientation, or polarizability of the neutral reagent, have been taken as evidence that collision dynamics

TABLE 2: Reaction Efficiencies^a (Eff.) and Primary Product Branching Ratios^b for Reactions of Charged Radicals 2–4 with Tetrahydrofuran, *tert*-Butyl Isocyanide, Toluene, and Phenol

	 2	 3	 4
	H abs ^c 100% Eff. = 76%	H abs 100% Eff. = 38%	H abs 81% CH ₂ abs 8% C ₂ H ₃ abs 6% CHO abs 3% C ₂ H ₃ O abs 2% Eff. = 28%
	CN abs 94% (2°) C ₄ H ₈ abs HCN abs 6% (2°)C ₄ H ₈ abs Eff. = 93%	CN abs 94% (2°) C ₄ H ₈ abs HCN abs 4% Eff. = 86%	HCN abs 64% (2°) HCN abs (2°) C ₄ H ₈ abs CN abs 36% Eff. = 90%
	adduct – H 42% adduct – CH ₃ 49% H abs 9% Eff. = 81%	adduct – H 55% adduct – CH ₃ 40% H abs 5% Eff. = 51%	adduct – H 36% adduct – CH ₃ 39% H abs 25% Eff. = 56%
	adduct – H 58% adduct – OH 39% H abs 3% Eff. = 83%	adduct – H 56% adduct – OH 42% H abs 2% Eff. = 65%	adduct – H 27% adduct – OH 62% H abs 11% Eff. = 54%

^a Reaction efficiencies are reported as $k_{\text{exp}}/k_{\text{coll}} \times 100\%$. ^b Secondary products are indicated as (2°) and are listed under the primary products that produce them. ^c abs = abstraction.

TABLE 3: Calculated Reaction Enthalpies (kcal/mol) for Abstraction Reactions by Charged Radicals 2–4 with Neutral Reagents^a

	 2	 3	 4
methanol ^b	-24.3	-24.1	-21.0
ethanol ^b	-25.6	-25.4	-22.3
dimethyl disulfide ^c	-37.1	-34.2	-36.6
cyclohexane ^d	-21.2	-21.0	-18.0

^a Calculated at the G3MP2B3 level of theory. ^b Abstraction of a hydrogen atom from the α -carbon atom to produce pyridinium cation and the α -dehydroalkanol. ^c Abstraction of an SCH₃ group to produce thiomethylpyridinium cation and thiomethyl radical. ^d Abstraction of a hydrogen atom to produce pyridinium cation and cyclohexyl radical.

do not play a role in determining the rates for these reactions.^{18,36,39,40} In the ion–molecule collision complexes, the ion and molecule can “swim” around one another in such a manner that the entire potential energy surface is explored. As a result, charged phenyl radicals display substituent effects similar to those observed in solution.

The reactions of charged phenyl radicals similar to 2–4 with several neutral reagents have been well-characterized. For example, charged phenyl radicals similar to 2–4 react with methanol, ethanol, tetrahydrofuran, isopropyl alcohol, and cyclohexane by hydrogen atom abstraction,^{18,41} with allyl iodide mainly by iodine atom abstraction,¹⁸ with dimethyl disulfide by thiomethyl (SCH₃) abstraction,³⁶ with *tert*-butyl isocyanide by CN abstraction,^{18c,e,42} and with toluene via a combination of hydrogen atom abstraction and addition/elimination pathways.³⁹ The observed trends in reaction efficiencies for various charged phenyl radicals reacting with the same neutral reagent via the

same pathways have been proposed to result from polar effects.⁴³ That is, as the electrophilicity of the charged phenyl radical increases, the transition states for its reactions become more polar, the transition state energy is lowered, and the reaction efficiency increases.

Interestingly, the reactivity of the charged phenyl radicals 2–4 can be classified into two groups: “regular” reactivity (Table 1), in which the reaction products and reactivity ordering (2 > 3 > 4) are consistent with previous studies⁴² on related charged phenyl radicals, and “irregular” reactivity (Table 2), in which anomalous reaction products or reaction efficiencies are observed. In the following discussion, the “regular” reactivity of 2–4 is considered first, followed by the “irregular” reactivity.

“Regular” Reactivity of Charged Radicals 2–4 toward Dimethyl Disulfide, Allyl Iodide, Cyclohexane, Methanol, Ethanol, 1-Pentanol, and Pyridine. All three charged radicals, 2–4, react with dimethyl disulfide mainly by thiomethyl (SCH₃)

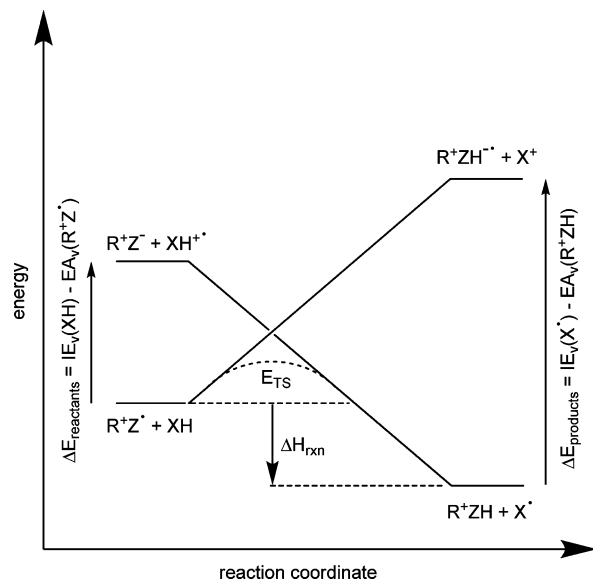


Figure 1. Hypothetical ionic avoided curve-crossing diagram illustrating the transition state for hydrogen atom abstraction from a hydrogen atom donor (XH) by an electrophilic radical (R^+Z^\bullet). The difference in the vertical ionization energy (IE_v) of the hydrogen atom donor and the EA_v of the radical (i.e., $\Delta E_{\text{reactants}}$), and the difference in the EA_v of the radical (R^+ZH) and the IE_v of the hydrogen atom donor (X^\bullet) after hydrogen atom abstraction (i.e., $\Delta E_{\text{products}}$), determine the energy of the ionic surface and, consequently, the barrier height (E_{TS}).

abstraction, with allyl iodide mainly by iodine atom abstraction and with cyclohexane, methanol, ethanol, and 1-pentanol exclusively by hydrogen atom abstraction (Table 1). Although the hydrogen and iodine atom abstraction reactions are likely to occur via a radical mechanism, SCH_3 abstraction from dimethyl disulfide may occur via either a radical or nonradical (e.g., nucleophilic addition/elimination) mechanism. Either mechanism would be expected to yield identical products, but it seems likely that a radical mechanism is operative in this case, since alkyl disulfides are known⁴⁴ to react with radicals via a stepwise S_H2 mechanism. The parameters that control the efficiencies of these reactions are discussed below.

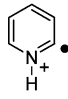
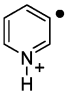
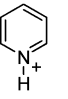
Reaction Enthalpies. Evans and Polanyi⁴⁵ were the first to propose a correlation between reaction enthalpy and barrier height, and this idea was further developed by Marcus to explain electron transfer⁴⁶ and atom abstraction reactions.⁴⁷ However, the calculated reaction enthalpies (ΔH_{rxn}) associated with the hydrogen atom abstraction reactions of charged radicals **2–4** with methanol and ethanol (Table 3) do not reflect the observed differences in the reaction rates with these two neutral reagents.

For example, ΔH_{rxn} for hydrogen atom abstraction from the α -carbon in ethanol⁴⁸ by **2** is only 0.2 and 3.3 kcal/mol more exothermic than those for **3** and **4**, respectively (ΔH_{rxn} ; -25.6 , -25.4 , and -22.3 kcal/mol, respectively; Table 3), yet the reaction efficiency for hydrogen atom abstraction by **2** (33%; Table 1) differs from that of **3** (11%) by a factor of 3 and from that of **4** (4.2%) by a factor of about 8. Similar trends are also observed for methanol (Tables 1 and 3). Interestingly, although the homolytic C–H bond dissociation energies at the α -carbon in ethanol and methanol are the same within experimental error,⁴⁹ all three charged radicals abstract a hydrogen atom from ethanol more efficiently than from methanol, and in the case of **4**, the difference is about an order of magnitude (Table 1).

Similar observations have been made earlier. For example, Donahue and co-workers showed for hydrogen atom abstraction from ethane by a series of radicals that the barrier heights vary from ~ 10 to ~ 0 kcal/mol, even when there is essentially no difference in the reaction enthalpies.⁴³ Similar results were obtained by Heberger and Lopata for the addition of carbon- and sulfur-centered radicals to vinyl groups.⁵⁰ In this case, reaction enthalpy was found to play a key role only for relatively nonpolar radicals, whereas polar effects were found to dominate for strongly nucleophilic or electrophilic radicals.

Polar Effects. Polarization of the transition state (i.e., increasing the degree of charge transfer) has been suggested to significantly influence the reactivity of electrophilic and nucleophilic radicals (i.e., the more polar the transition state, the lower its energy and, consequently, the faster the reaction).⁴³ The ionic avoided curve-crossing model developed by Anderson and co-workers⁵¹ has been used previously to explain relative rates of radical reactions like the ones reported here.^{18,41} In this model, which is a slightly modified version of the valence-bond avoided curve-crossing model developed by Shaik et al.,⁵² the barrier height of a radical-molecule reaction is defined on the basis of an avoided crossing of the ground state and a hypothetical ionic excited state of the reactants (instead of the triplet state proposed by Shaik et al.) having the same geometry. The development of this model was motivated by the observation that the transition state energy correlates directly with the ionic energy of the separated reactants, which is expressed as the difference ($\Delta E_{\text{reactants}}$) in the vertical ionization energy (IE_v) of the hydrogen atom donor⁵³ and the EA_v of the radical reactant. For a positively charged radical (such as those studied here), R^+Z^\bullet , and a neutral reagent, XH, the hypothetical ionic excited state can be represented as $[R^+Z^-][XH^+]$.^{43,51,52,54} Increasing the electron affinity of the charged radical or decreasing the ionization energy of the neutral reagent stabilizes this configuration. A general ionic avoided curve-crossing diagram for the

TABLE 4: Calculated Activation Enthalpies^a (kcal/mol) for Hydrogen Atom Abstraction by Charged Radicals **2–4 from Methanol and Ethanol^{b,c}**

			
	2	3	4
methanol	-9.8 (-10.6)	-4.0 (-4.5)	-2.4 (-2.9)
ethanol	-12.7 (-13.1)	-6.5 (-5.9)	-4.7 (-4.3)

^a "Activation enthalpy" is the difference in enthalpy between the separated reactants and the transition state. ^b Abstraction of a hydrogen atom from the α -carbon atom to produce pyridinium cation and the α -dehydroalcohol. ^c Calculated at the G3MP2B3 level of theory; values in parentheses calculated at the MPW1K/6-31+G(d,p) level of theory.

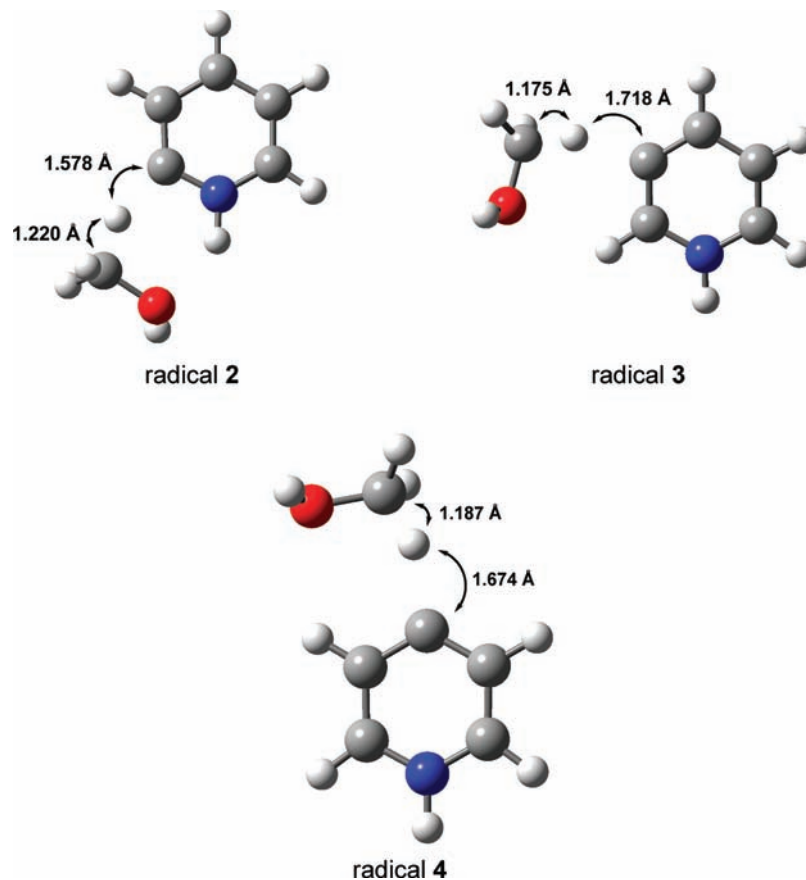


Figure 2. Calculated (G3MP2B3) transition-state structures for hydrogen atom abstraction from methanol by charged radicals 2–4. The distances between the hydrogen atom being transferred and the α -carbon atom in methanol are 1.220, 1.175, and 1.187 Å, respectively. The distances between the hydrogen atom being transferred and the radical site are 1.578, 1.718, and 1.674 Å, respectively.

case described above where the reactant radical is electrophilic and the product radical is nucleophilic is shown in Figure 1.

Barrier Heights. The calculated (G3MP2B3 and MPW1K) activation enthalpies (i.e., the difference in enthalpy between the separated reactants and the transition state) for hydrogen atom abstraction from methanol and ethanol by charged radicals 2–4 (Table 4) parallel the observed reaction efficiencies (Table 1). Because the G3MP2B3 method has not been extensively tested (calibrated) for barrier heights, transition state calculations were also performed by using the MPW1K method, which has been optimized to give the best fit to kinetic data for 40 radical reactions.³² Interestingly, at these two levels of theory, the calculated activation enthalpies differ by only 0.4–0.8 kcal/mol (Table 4). It should be noted that all of the activation enthalpy values are negative due to the formation of a gas-phase collision complex stabilized by ion-dipole and ion-induced dipole forces prior to reaction of the ion with the neutral molecule. The calculated (G3MP2B3) transition state structures for methanol are shown in Figure 2. For these transition states, the distances between the hydrogen atom being transferred and the α -carbon in methanol (1.220, 1.175, and 1.187 Å for 2–4, respectively) are much shorter than the distances between the hydrogen atom being transferred and the radical site (1.578, 1.718, and 1.674 Å for 2–4, respectively). The calculated distances for the transition states of ethanol are similar. Hence, the structures of the transition states are closer to those for the reactants than those for the products; that is, they are “early” transition states. Further, because all of the (calculated) reaction enthalpies (ΔH_{rxn}) for hydrogen atom abstraction from either methanol or ethanol by 2–4 have large negative values (Table 3), “early” transition states are expected for all of these reactions.

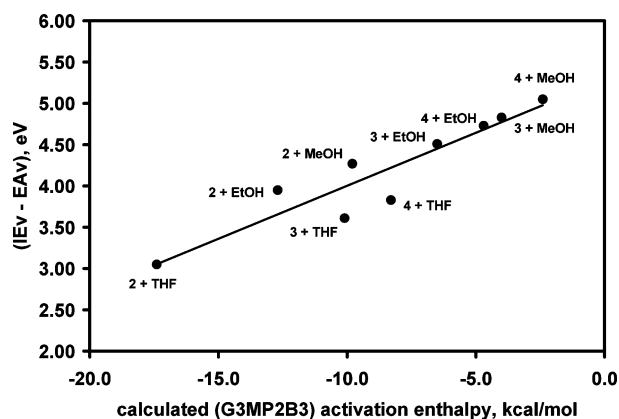
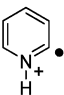
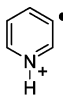
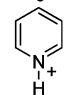


Figure 3. Calculated ($\text{IE}_v - \text{EA}_v$) values (eV) versus calculated (G3MP2B3) activation enthalpies (kcal/mol) for hydrogen atom abstraction from methanol (MeOH), ethanol (EtOH), and tetrahydrofuran (THF) by charged radicals 2–4.

As a result, the barrier heights for these reactions should correlate with the difference in energy between IE_v for methanol and ethanol and EA_v for 2–4 ($\Delta E_{\text{reactants}}$, Figure 1). Indeed, a good correlation exists between the calculated ($\text{IE}_v - \text{EA}_v$) values and the calculated activation enthalpies for hydrogen atom abstraction from methanol, ethanol and THF (discussed below) by 2–4 (Figure 3).

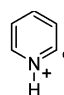
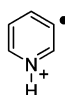
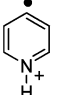
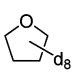
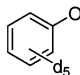
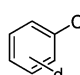
The trends in the reaction efficiencies (i.e., $2 > 3 > 4$) for hydrogen atom abstraction from methanol and ethanol by 2–4 also parallel the calculated ($\text{IE}_v - \text{EA}_v$) values (Table 5). This observation is consistent with previous studies on hydrogen atom abstraction by charged phenyl radicals with a variety of

TABLE 5: Calculated Values for $(IE_v - EA_v)$ and Measured Hydrogen Atom Abstraction Efficiencies^a (Eff.) for Reactions of Charged Radicals 2–4 with Methanol and Ethanol

			
	2	3	4
	$EA_v = 6.69 \text{ eV}^b$	$EA_v = 6.13 \text{ eV}^b$	$EA_v = 5.91^b$
methanol $IE_v = 10.96 \text{ eV}^c$	$(IE_v - EA_v) = 4.27 \text{ eV}$ Eff. = 21%	$(IE_v - EA_v) = 4.83 \text{ eV}$ Eff. = 1.7%	$(IE_v - EA_v) = 5.05 \text{ eV}$ Eff. = 0.4%
ethanol $IE_v = 10.64 \text{ eV}^d$	$(IE_v - EA_v) = 3.95 \text{ eV}$ Eff. = 33%	$(IE_v - EA_v) = 4.51 \text{ eV}$ Eff. = 11%	$(IE_v - EA_v) = 4.73 \text{ eV}$ Eff. = 4.2%

^a Reaction efficiencies are reported as $k_{\text{exp}}/k_{\text{coll}} \times 100\%$. ^b Calculated at the B3LYP/aug-cc-pVTZ//B3LYP/cc-pVTZ level of theory. ^c Ref 55. ^d Ref 56.

TABLE 6: Reaction Efficiencies^a (Eff.) and Primary Product Branching Ratios for Reactions of Charged Radicals 2–4 with Tetrahydrofuran-*d*₈, Phenol-*d*₅, and Toluene-*d*₅

			
	2	3	4
	not studied	not studied	D abs 68% CD ₂ abs 20% CDO + C ₂ D ₃ abs 10% C ₂ D ₃ O abs 2% Eff. = 26%
	adduct - D 29% adduct - OH 61% adduct 9% H abs 1% Eff. = 48%	adduct - D 25% adduct - OH 74% H abs 1% Eff. = 36%	adduct - D 10% adduct - OH 83% D abs 7% Eff. = 33%
	adduct 3% adduct - D 16% adduct - CH ₃ 70% H abs 11% Eff. = 65%	adduct - D 21% adduct - CH ₃ 73% H abs 6% Eff. = 43%	adduct - D 17% adduct - CH ₃ 55% D abs 26% H abs 2% Eff. = 56%

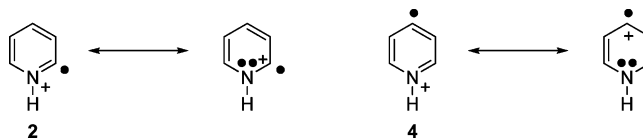
^a Reaction efficiencies are reported as $k_{\text{exp}}/k_{\text{coll}} \times 100\%$.

hydrogen atom donors.⁴¹ Charged radicals **2–4** react more rapidly with ethanol than with methanol because the IE_v for ethanol is about 0.32 eV lower than that for methanol, and this causes $(IE_v - EA_v)$ to be smaller for ethanol than methanol (Table 5).

“Irregular” Reactivity of Charged Radicals 2–4 toward Tetrahydrofuran, *tert*-Butyl Isocyanide, Toluene, and Phenol. The reactions of charged radicals **2–4** with THF, *tert*-butyl isocyanide, toluene, and phenol (Table 2) yield some rather unusual (and unexpected) products. The reactions with THF will be considered first. Although **2** and **3** react with THF exclusively by hydrogen atom abstraction, **4** undergoes other reactions (in addition to hydrogen atom abstraction) that represent ~20% of the product distribution (Table 2). These minor products were identified to arise from net abstraction of CH₂, C₂H₃, CHO, or C₂H₃O by determining their exact masses and by examining the reaction of **4** with perdeuterated THF (Table 6).

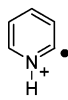
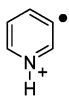
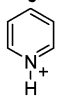
For radical **4**, the products that are not a result of hydrogen atom abstraction are likely to arise from initial nucleophilic addition of THF to the dehydrocarbon atom (the most electron-deficient carbon atom) rather than from radical attack on THF,

since neither synchronous nor stepwise S_H2 reactions are known to occur at an sp³ carbon atom (with the exception of strained ring systems) or an sp³ oxygen atom (with the exception of peroxides).⁴³ Nucleophilic addition of THF to the dehydrocarbon atom of **4** can be rationalized by considering its ionized carbene-type resonance structure (which permits greater charge delocalization away from the nitrogen atom). This type of resonance structure also exists for radical **2**, but not for radical **3**.



The calculated (G3MP2B3) reaction enthalpies for addition of THF to the radical site in charged radicals **2–4** are -12.3, -16.9, and -17.8 kcal/mol, respectively. Although all of these reactions are calculated to be exothermic, the barrier heights for addition of THF to both **2** and **4** are calculated to be

TABLE 7: Calculated Activation Enthalpies^a (kcal/mol) for Hydrogen Atom Abstraction and Addition by Charged Radicals 2–4 with Tetrahydrofuran^b

			
	2	3	4
H-atom abstraction ^c	-17.4 (-17.1)	-10.1 (-8.6)	-8.3 (-6.9)
addition ^d	-11.9	-5.1	-14.3

^a “Activation enthalpy” is the difference in enthalpy between the separated reactants and the transition state. ^b Calculated at the G3MP2B3 level of theory; values in parentheses calculated at the MPW1K/6-31+G(d,p) level of theory. ^c Abstraction of a hydrogen atom to produce pyridinium cation and α -dehydrotetrahydrofuran. ^d Addition of tetrahydrofuran to the radical to produce adduct.

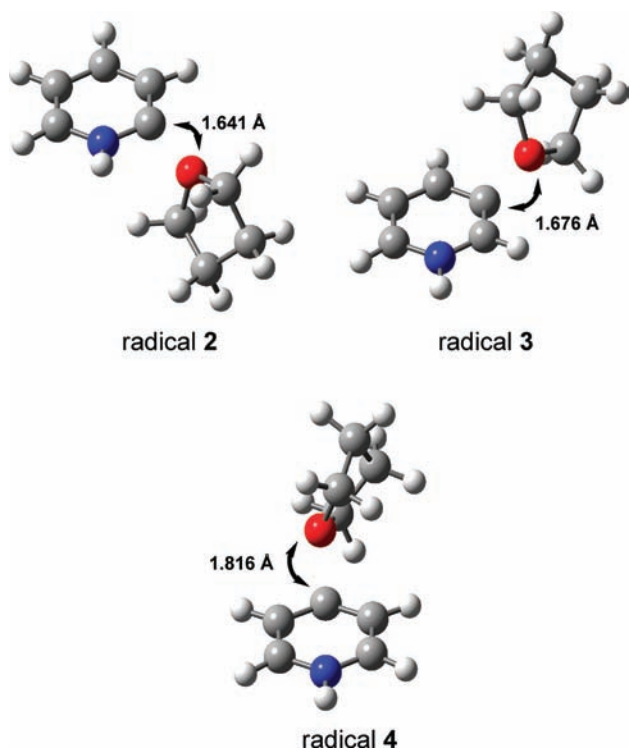


Figure 4. Calculated (G3MP2B3) transition-state structures for addition of tetrahydrofuran to charged radicals 2–4. The distances between the oxygen atom and the dehydrocarbon atom are 1.641, 1.676, and 1.816 Å, respectively.

significantly lower than that for **3** (−11.9, −5.1, and −14.3 kcal/mol for **2–4**, respectively; Table 7). The calculated (G3MP2B3) transition state structures are shown in Figure 4. A comparison of the calculated barrier heights for addition of THF with those for hydrogen atom abstraction from THF by **2–4** (−17.4, −10.1, and −8.3 kcal/mol, respectively (G3MP2B3); Table 7) indicates that the barrier for addition of THF to both **2** and **3** is sufficiently high that addition cannot compete (kinetically) with hydrogen atom abstraction. The calculated (G3MP2B3) transition state structures for hydrogen atom abstraction from THF by **2–4** are shown in Figure 5. Both **2** and **3** react with THF only by hydrogen atom abstraction (Table 2). Even though **2** possesses an ionized carbene-type resonance structure (like **4**), which might be expected to facilitate nucleophilic addition, it appears that this is overcome by the ability of the charge site to catalyze hydrogen atom abstraction because THF can interact simultaneously with both the charge and radical sites. The transition state structure for **2** (Figure 5) shows a hydrogen-bonding interaction between the oxygen atom of THF and the N–H

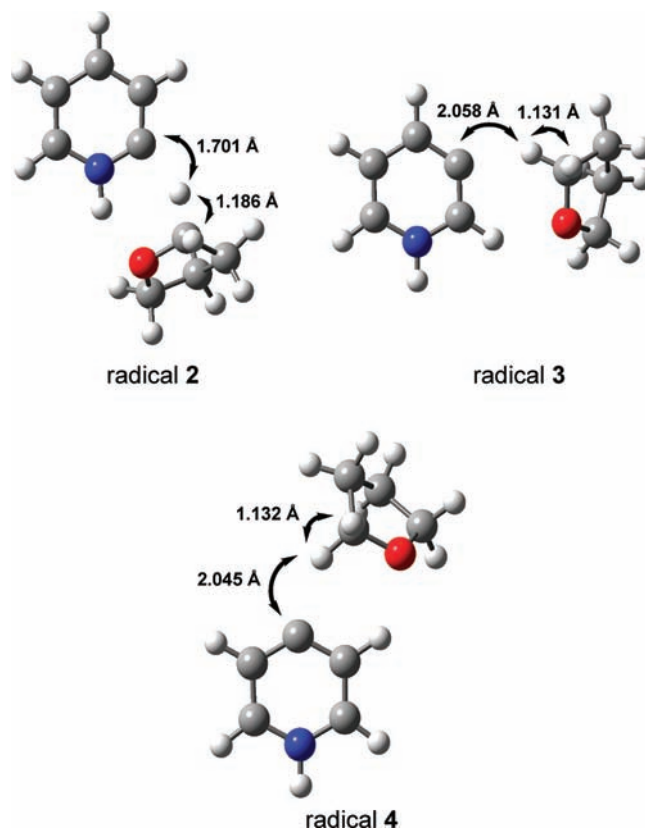
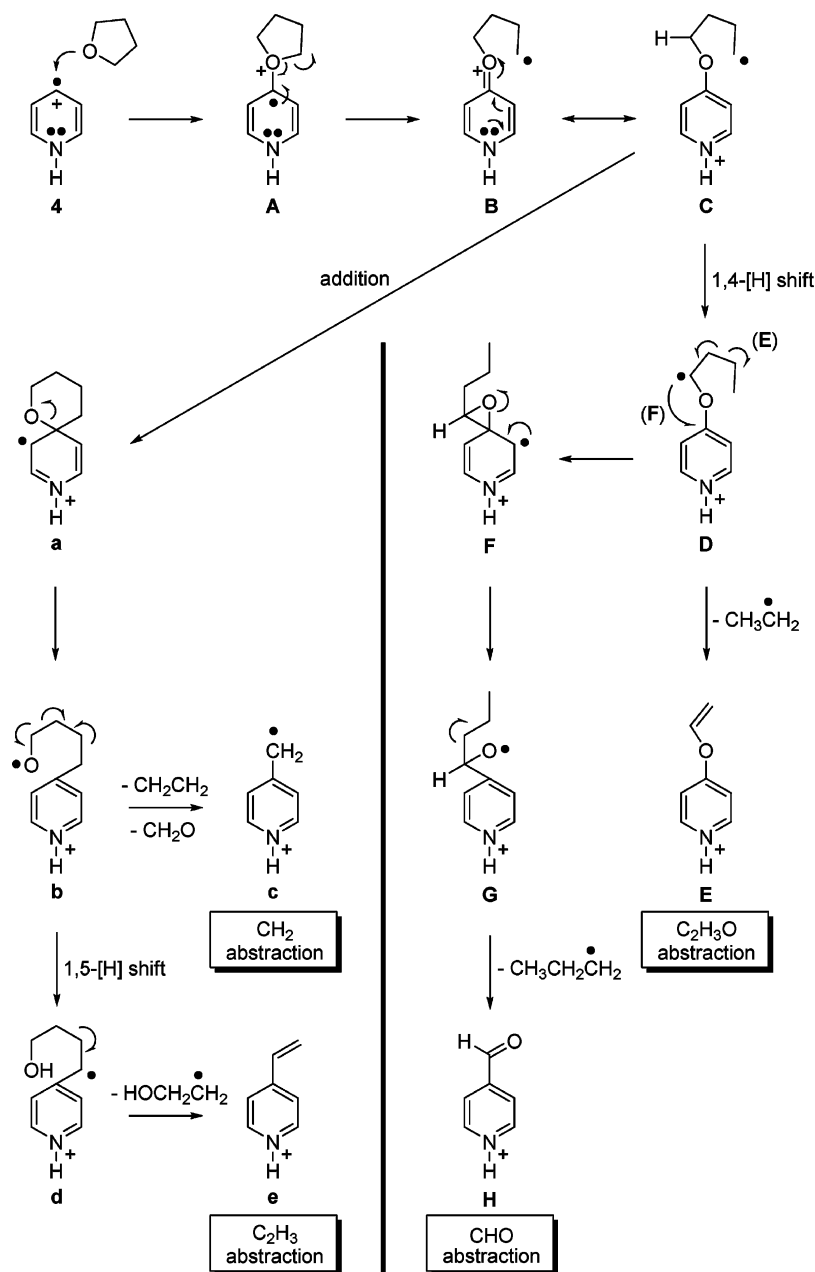


Figure 5. Calculated (G3MP2B3) transition-state structures for hydrogen atom abstraction from tetrahydrofuran by charged radicals 2–4. The distances between the hydrogen atom being transferred and the α -carbon atom in tetrahydrofuran are 1.186, 1.131, and 1.132 Å, respectively. The distances between the hydrogen atom being transferred and the radical site are 1.701, 2.058, and 2.045 Å, respectively.

proton that likely provides additional stabilization and, hence, biases **2** toward hydrogen atom abstraction. The observation that hydrogen atom abstraction dominates over nucleophilic addition for **4**, despite the fact that the barrier for the former is calculated to be significantly higher than for the latter, is at least partially explained by entropy; that is, there are a greater number of identical, or nearly identical, transition state structures for hydrogen atom abstraction than for nucleophilic addition due to the four essentially identical α -hydrogen atoms in THF.

Possible pathways for the formation of the CH_2 , CHO , C_2H_3 , and $\text{C}_2\text{H}_3\text{O}$ (net) abstraction products from the reaction of **4** with THF are shown in Scheme 1.⁵⁷ All of these reactions are calculated (G3MP2B3) to be exothermic (ΔH_{rxn} : −9.6, −19.0, −16.9, and −15.2 kcal/mol, respectively). Upon addition of THF to the dehydrocarbon atom of **4**, the odd spin is delocalized in

SCHEME 1



the pyridinium π -system (A; Scheme 1). The odd spin may catalyze ring-opening of THF via α -cleavage (C; Scheme 1). Ethyl radical loss to form the net C₂H₃O abstraction product must involve a hydrogen-atom shift to form an ethyl group. We propose that a 1,4-hydrogen shift in the ring-opened adduct (D; Scheme 1) followed by another α -cleavage leads to the loss of an ethyl radical, resulting in net C₂H₃O abstraction (E; Scheme 1). Since radicals readily add to aromatic rings, it is logical to assume that the alkyl radical formed upon the above ring-opening and 1,4-hydrogen shift (D; Scheme 1) may add to the π -system of the phenyl ring (F; Scheme 1), followed by α -cleavage (G; Scheme 1), to yield an oxygen-centered radical that can eliminate a propyl radical to produce the (net) CHO abstraction product (H; Scheme 1).

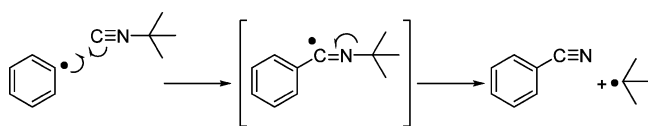
If, however, the carbon-centered radical formed upon ring-opening of the THF adduct (C; Scheme 1) adds to the π -system of the aromatic ring (a; Scheme 1) instead of undergoing a 1,4-hydrogen shift, then the resulting spiro compound may undergo subsequent ring-opening to form an oxygen-centered radical (b;

Scheme 1). This intermediate is poised to lose formaldehyde and ethylene to generate the (net) CH₂ abstraction product (c; Scheme 1). The oxygen-centered radical (b; Scheme 1) may also undergo a 1,5-hydrogen shift to form a delocalized benzyl radical (d; Scheme 1), which can then fragment to yield the (net) C₂H₃ abstraction product (e; Scheme 1).

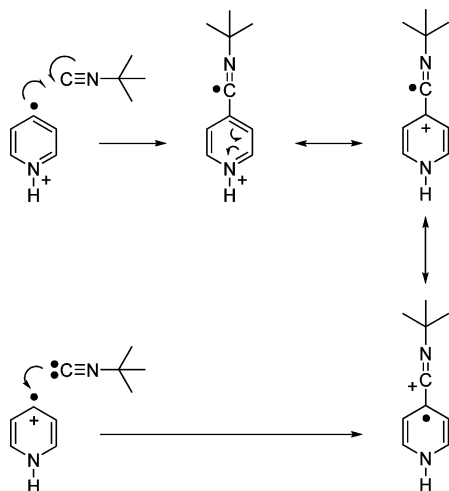
On the basis of this proposed mechanism, the (net) CH₂ abstraction product can be formed without the need for a hydrogen atom shift, as opposed to several of the other reactions. Thus, the rate of formation of this product should be insensitive to primary deuterium isotope effects. Indeed, reaction of **4** with perdeuterated THF (Table 6) results in an increased formation of the CH₂ abstraction product at the expense of the other products, which lends support to the proposed mechanism.

The reactions of charged radicals **2–4** with *tert*-butyl isocyanide are now considered. The phenyl radical is known to add to the “carbenoid” *tert*-butyl isocyanide via an imidoyl intermediate to produce benzonitrile (net CN abstraction) and *tert*-butyl radical (Scheme 2).⁵⁰ Charged phenyl radicals have

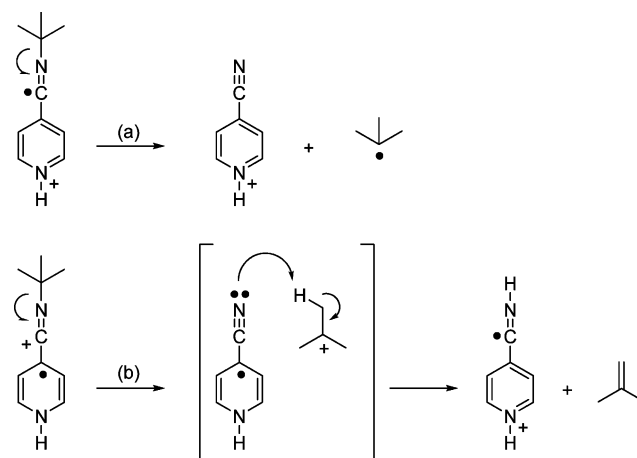
SCHEME 2



SCHEME 3



SCHEME 4



been shown to react in the same manner.^{18c,39} Whereas (net) CN abstraction is the major product for the reaction of both **2** and **3** with *tert*-butyl isocyanide (94% and 94%, respectively; Table 2), (net) HCN abstraction is the major product for **4** (64%; Table 2). Again, the ionized carbene-type resonance structure for **4** may be responsible, at least in part, for its unusual reactivity with *tert*-butyl isocyanide. Unfortunately, though, no mechanistic information can be gleaned from the experimental observations, since both possible mechanisms for the reaction of **4** with *tert*-butyl isocyanide (i.e., nucleophilic addition by

tert-butyl isocyanide and radical addition by **4**; Scheme 3) produce the same imidoyl intermediate. Therefore, the nature of charge and spin delocalization in the intermediate (rather than the pathway that leads to the intermediate) is likely the determining factor for whether (net) CN or HCN abstraction occurs.

To explore the spin and charge distributions in these intermediates, B3LYP/cc-pVDZ//B3LYP/6-31G(d) calculations were performed for the imidoyl intermediates that are formed in the reaction of *tert*-butyl isocyanide with charged radicals **2**–**4**. These intermediates possess resonance structures that delocalize the charge and odd spin over every atom in the pyridine ring. The calculated spin and charge distributions for the three imidoyl intermediates (**2I**–**4I**) are shown in Figure 6. For **4I**, the α -spin density is distributed over every heavy atom, but there is relatively little α -spin density on the benzylic carbon atom. In contrast, the intermediates resulting from addition of

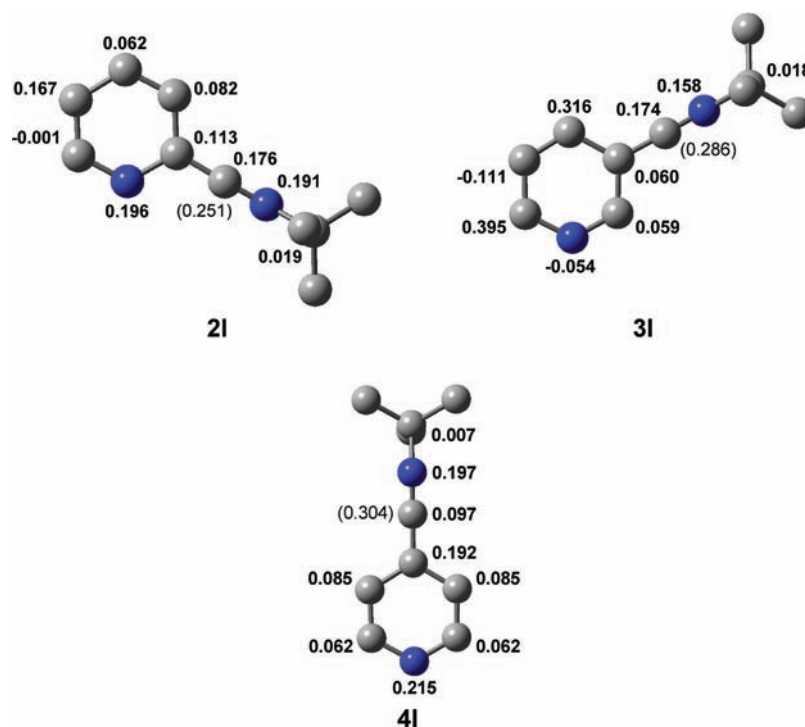
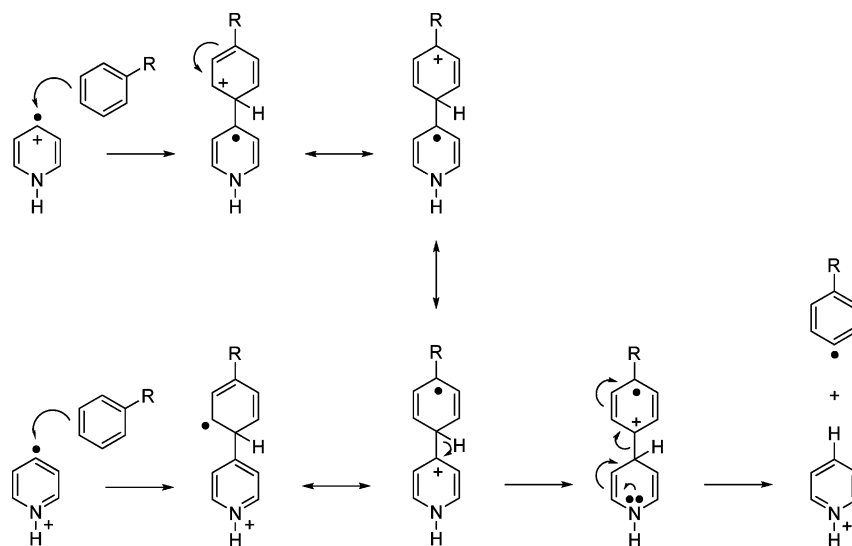


Figure 6. Calculated (B3LYP/cc-pVDZ//B3LYP/6-31G(d)) spin densities (Mulliken) for the heavy atoms in the intermediates formed from addition of *tert*-butyl isocyanide to charged radicals **2**–**4**. Positive and negative values correspond to α - and β -spin densities, respectively. Calculated atomic charges for the benzylic carbon atoms are shown in parentheses.

SCHEME 5



tert-butyl isocyanide to **2** and **3** (**2I** and **3I**; Figure 6) have significantly more α -spin density on the benzylic carbon atom. Greater α -spin density on the benzylic carbon atom would be expected to facilitate the homolytic bond cleavage that leads to the loss of a *tert*-butyl radical and (net) CN abstraction (Scheme 4, pathway a). On the other hand, the larger atomic charge on the benzylic carbon atom of **4I** may facilitate an initial heterolytic cleavage in the intermediate, followed by proton transfer in the complex to yield the final (net) HCN abstraction product (Scheme 4, pathway b).

Finally, the reactions of charged radicals **2–4** with toluene and phenol are considered. Interestingly, the overall reaction efficiencies for **2–4** with toluene (Table 2) do not follow the trend (i.e., **2** > **3** > **4**) predicted by the ionic avoided curve-crossing model. Instead, the overall reaction efficiencies for **3** and **4** (51% and 56%, respectively; Table 2) are about the same, and they are significantly lower than that for **2** (81%; Table 2). In addition, **4** abstracts a hydrogen atom from toluene substantially faster than either **2** or **3** (Table 2). Relatively fast hydrogen atom abstraction was also observed for the reactions of **4** with phenol (Table 2). Examination of the reactions of **2–4** with phenol-*d*₅ and toluene-*d*₅ (Table 6) revealed that whereas **2** and **3** abstract only hydroxyl and methyl hydrogen atoms from phenol-*d*₅ and toluene-*d*₅, respectively, **4** almost exclusively abstracts a deuterium atom from the aromatic ring. Possible pathways for this reaction involve either an electrophilic or radical addition to the aromatic ring, rearrangement by a 1,2-hydride shift, and subsequent fragmentation (Scheme 5). In support of this mechanism, a substantial primary isotope effect is associated with this reaction (Tables 2 and 6). The same was observed for addition followed by elimination of a deuterium atom, as expected. Again, different spin and charge distributions for the intermediates of **4**, as compared to those of **2** and **3**, may be responsible for this reactivity, although these were not studied computationally.

Conclusions

The results reported here provide the first comparison of the reactivity of the three isomeric dehydropyridinium cations with the goal of elucidating the effects of the electronic structure of charged radicals on their radical reactivity. The relative rates for hydrogen atom abstraction by the three radicals from methanol, ethanol, 1-pentanol and cyclohexane, thiomethyl

abstraction from dimethyl disulfide; and iodine atom abstraction from allyl iodide parallel their calculated electron affinities, as expected for reactions of polar radicals.

For **4**, unusual reactivity was observed with several neutral reagents. For example, whereas **2** and **3** show only hydrogen atom abstraction from THF, **4** reacts with THF to yield products arising from nonradical reactivity (in addition to hydrogen atom abstraction). An ionized carbene-type resonance structure is likely responsible, at least in part, for the nonradical reactivity observed for **4**. This ionized carbene-type resonance structure permits greater charge delocalization away from the nitrogen atom and, as a consequence, facilitates nucleophilic addition to the most electrophilic carbon atom (C-4). Charged radical **2** also possesses an ionized carbene-type resonance structure, but nonradical reactivity toward THF was not observed for this molecule. For **2**, the barrier height for hydrogen atom abstraction is calculated to be lower than that for addition, which is a result of a stabilizing hydrogen-bonding interaction in the transition state.

Finally, whereas charged radicals **2** and **3** react with *tert*-butyl isocyanide predominantly by CN abstraction, **4** reacts predominantly by HCN abstraction. Charged radical **4** also undergoes a rather surprising hydrogen atom abstraction from the phenyl ring of toluene and phenol, while **2** and **3** abstract a hydrogen atom from the hydroxyl and methyl groups in these reagents. The unusual reactivity of **4** toward *tert*-butyl isocyanide, toluene, and phenol is likely due to the nature of charge and spin delocalization in the intermediates that are formed rather than the pathway that leads to the intermediates.

Acknowledgment. We thank Purdue University and General Electric for a Predoctoral Fellowship (A.A.). Financial support by the National Institutes of Health is also gratefully acknowledged.

Supporting Information Available: Tables of Cartesian coordinates, electronic energies, zero-point vibrational energies, 298 K thermal contributions, and derived enthalpies for all species. Complete ref 35. This material is available free of charge via the Internet at <http://pubs.acs.org>.

References and Notes

- (1) See, for example: (a) Donahue, N. M. *Chem. Rev.* **2003**, *103*, 4593. (b) Pardo, L.; Banfelder, J. R.; Osman, R. *J. Am. Chem. Soc.* **1992**, *114*,

2382. (c) Tiu, G. C.; Tao, F.-M. *Chem. Phys. Lett.* **2006**, *428*, 42. (d) Roberts, B. P. *Chem. Soc. Rev.* **1999**, *28*, 25. (e) Chen, Y.; Tschuikow-Roux, E. *J. Phys. Chem.* **1993**, *97*, 3742. (f) Galano, A.; Alvarez-Idaboy, J. R.; Bravo-Pérez, G.; Ruiz-Santoyo, M. E. *Phys. Chem. Chem. Phys.* **2002**, *4*, 4648. (g) Blowers, P.; Masel, R. *AIChE J.* **2000**, *46*, 2041. (h) Strong, H. L.; Brownawell, M. L.; San Filippo, J., Jr. *J. Am. Chem. Soc.* **1983**, *105*, 6526. (i) Mebel, A. M.; Lin, M. C.; Yu, T.; Morokuma, K. *J. Phys. Chem. A* **1997**, *101*, 3189.
- (2) Kraka, E.; Cremer, D. *J. Am. Chem. Soc.* **2000**, *122*, 8245.
- (3) Griffiths, J.; Murphy, J. A. *J. Chem. Soc. Chem. Commun.* **1991**, 1422.
- (4) Wender, P. A.; Jeon, R. *Org. Lett.* **1999**, *1*, 2117.
- (5) Wender, P. A.; Jeon, R. *Bioorg. Med. Chem. Lett.* **2003**, *13*, 1763.
- (6) Griffiths, J.; Murphy, J. A. *J. Chem. Soc. Chem. Commun.* **1992**, 24.
- (7) Hoffner, J.; Schottelius, M. J.; Feichtinger, D.; Chen, P. *J. Am. Chem. Soc.* **1998**, *120*, 376.
- (8) Chen, P. *Angew. Chem., Int. Ed., Engl.* **1996**, *35*, 1478.
- (9) Greenley, T. L.; Davies, M. J. *Biochim. Biophys. Acta* **1993**, *1157*, 23.
- (10) Hazlewood, C.; Davies, M. J. *Arch. Biochem. Biophys.* **1996**, *332*, 79.
- (11) Meunier, B.; Pratiel, G.; Bernadou, J. *Bull. Soc. Chim. Fr.* **1994**, *131*, 933.
- (12) Nicolaou, K. C.; Dai, W. M. *Angew. Chem., Int. Ed.* **1991**, *30*, 1387.
- (13) Pratiel, G.; Bernadou, J.; Meunier, B. *Angew. Chem., Int. Ed., Engl.* **1995**, *34*, 746.
- (14) Dean, R. T.; Fu, S.; Stocker, R.; Davies, M. J. *Biochem. J.* **1997**, *324*, 1. (b) Pogozelski, W. K.; Tullius, T. D. *Chem. Rev.* **1998**, *98*, 1089.
- (15) (a) Sander, W. *Acc. Chem. Res.* **1999**, *32*, 669. (b) Wenk, H. H.; Winkler, M.; Sander, W. *Angew. Chem., Int. Ed.* **2003**, *42*, 502.
- (16) (a) Bridger, R. F.; Russell, G. A. *J. Am. Chem. Soc.* **1963**, *85*, 3754. (b) Pryor, W. A.; Guard, H. J. *Am. Chem. Soc.* **1964**, *86*, 1150. (c) Fu, J.-J. L.; Bentrude, W. G. *J. Am. Chem. Soc.* **1972**, *94*, 7710. (d) Scavano, J. C.; Stewart, L. C. *J. Am. Chem. Soc.* **1983**, *105*, 3609. (e) Sommeling, P. M.; Mulder, P.; Louw, R.; Avila, D. V.; Luszyk, J.; Ingold, K. U. *J. Phys. Chem.* **1993**, *97*, 8362. (f) Yu, T.; Lin, M. C.; Melius, C. F. *Int. J. Chem. Kinet.* **1994**, *26*, 1095.
- (17) (a) Fahr, A.; Stein, S. E. *J. Phys. Chem.* **1988**, *92*, 4951. (b) Chen, R. H.; Kafafi, A.; Stein, S. E. *J. Am. Chem. Soc.* **1989**, *111*, 1418.
- (18) (a) Li, R.; Smith, R.; Kenttämaa, H. I. *J. Am. Chem. Soc.* **1996**, *118*, 5056. (b) Heidbrink, J. L.; Ramirez-Arizmendi, L. E.; Thoen, K. K.; Ferra, J. J.; Kenttämaa, H. I. *J. Phys. Chem. A* **2001**, *105*, 7875. (c) Tichy, S. E.; Thoen, K. K.; Price, J. M.; Ferra, J. J.; Petucci, C. J.; Kenttämaa, H. I. *J. Org. Chem.* **2001**, *66*, 2726. (d) Thoen, K.; Smith, R. L.; Nousiainen, J. J.; Nelson, E. D.; Kenttämaa, H. I. *J. Am. Chem. Soc.* **1996**, *118*, 8669. (e) Petucci, C.; Nyman, M.; Guler, L.; Kenttämaa, H. I. *J. Am. Chem. Soc.* **2002**, *124*, 4108. (f) Jing, L.; Guler, L. P.; Nash, J. J.; Kenttämaa, H. I. *J. Am. Chem. Soc. Mass Spectrom.* **2004**, *15*, 913. (g) Smith, R. L.; Thoen, K. K.; Stirk, K. M.; Kenttämaa, H. I. *Int. J. Mass Spectrom. Ion Processes* **1997**, *165/166*, 315.
- (19) (a) Lavorato, D. J.; Terlouw, J. K.; McGibbon, G. A.; Dargel, T. K.; Koch, W.; Schwarz, H. *Int. J. Mass Spectrom.* **1998**, *179*, 7. (b) Lavorato, D.; Terlouw, J. K.; Dargel, T. K.; Koch, W.; McGibbon, G. A.; Schwarz, H. *J. Am. Chem. Soc.* **1996**, *118*, 11898.
- (20) Gauthier, J. W.; Trautman, T. R.; Jacobson, D. B. *Anal. Chim. Acta* **1991**, *246*, 211.
- (21) Chen, L.; Wang, T. C. L.; Ricca, T. L.; Marshall, A. G. *Anal. Chem.* **1987**, *59*, 449.
- (22) Su, T.; Chesnavich, W. J. *J. Chem. Phys.* **1982**, *76*, 5183.
- (23) (a) Bartmess, J. E.; Georgiadis, R. M. *Vacuum* **1983**, *33*, 149. (b) Miller, K. J.; Savchik, J. A. *J. Am. Chem. Soc.* **1979**, *101*, 7206.
- (24) (a) Curtiss, L. A.; Raghavachari, K.; Redfern, P. C.; Rassolov, V.; Pople, J. A. *J. Chem. Phys.* **1998**, *109*, 7764. (b) Baboul, A. G.; Curtiss, L. A.; Redfern, P. C.; Raghavachari, K. *J. Chem. Phys.* **1999**, *110*, 7650.
- (25) Hariharan, P. C.; Pople, J. A. *Theor. Chim. Acta* **1973**, *28*, 213.
- (26) Becke, A. D. *J. Chem. Phys.* **1996**, *104*, 1040.
- (27) Lee, C.; Yang, W.; Parr, R. G. *Phys. Rev. B* **1988**, *37*, 785.
- (28) Dunning, T. H., Jr. *J. Chem. Phys.* **1989**, *90*, 1007.
- (29) Note that, for these calculations, we are computing the vertical electron affinity of the radical site, not the vertical electron affinity of the molecule.
- (30) Because the aryl radicals studied here contain a formal positive charge on the nitrogen atom, the state that is produced when an electron is added to the nonbonding orbital is formally zwitterionic; i.e., it contains localized positive (π) and negative (σ) charges.
- (31) Breneman, C. M.; Wiberg, K. B. *J. Comput. Chem.* **1990**, *11*, 361.
- (32) Lynch, B. J.; Fast, P. L.; Harris, M.; Truhlar, D. G. *J. Phys. Chem. A* **2000**, *104*, 4811.
- (33) Lynch, B. J.; Truhlar, D. G. *J. Phys. Chem. A* **2001**, *105*, 2936.
- (34) (a) Hehre, W. J.; Ditchfield, R.; Pople, J. A. *J. Chem. Phys.* **1972**, *56*, 2257. (b) Francl, M. M.; Pietro, W. J.; Hehre, W. J.; Binkley, J. S.; Gordon, M. S.; DeFrees, D. J.; Pople, J. A. *J. Chem. Phys.* **1982**, *77*, 3654. (c) Clark, T.; Chandrasekhar, J.; Schleyer, P. v. R. *J. Comput. Chem.* **1983**, *4*, 294. (d) Frisch, M. J.; Pople, J. A.; Binkley, J. S. *J. Chem. Phys.* **1984**, *80*, 3265.
- (35) Frisch, M. J., et al. *Gaussian 03, Revision B.03*, Gaussian, Inc.: Pittsburgh PA, 2003.
- (36) (a) Stirk, K. M.; Orłowski, J. C.; Leeck, D. T.; Kenttämaa, H. I. *J. Am. Chem. Soc.* **1992**, *114*, 8604. (b) Beasley, B. J.; Smith, R. L.; Kenttämaa, H. I. *J. Mass Spectrom.* **1995**, *30*, 384. (c) Thoen, K. K.; Beasley, B. J.; Smith, R. L.; Kenttämaa, H. I. *J. Am. Soc. Mass Spectrom.* **1996**, *7*, 1245.
- (37) (a) Lifshitz, C. *J. Phys. Chem.* **1982**, *86*, 606. (b) Leeck, D. T.; Kenttämaa, H. I. *Org. Mass Spectrom.* **1994**, *29*, 106.
- (38) This is generally true for gas-phase ion–molecule reactions (e.g., S_N2 reactions). For an excellent discussion, see: DePuy, C. H. *J. Org. Chem.* **2002**, *67*, 2393.
- (39) Ramirez-Arizmendi, L. E.; Guler, L.; Ferra, J. J., Jr.; Thoen, K. K.; Kenttämaa, H. I. *Int. J. Mass Spectrom.* **2001**, *210/211*, 511.
- (40) Petzold, C. J.; Nelson, E. D.; Lardin, H. A.; Kenttämaa, H. I. *J. Phys. Chem. A* **2002**, *106*, 9767.
- (41) Jing, L.; Nash, J. J.; Kenttämaa, H. I. *J. Am. Chem. Soc.* **2008**, *130*, 17697.
- (42) Nelson, E. D.; Li, R.; Kenttämaa, H. I. *Int. J. Mass Spectrom.* **1999**, *185*, 91–187.
- (43) See, for example: Pross, A. *Theoretical and Physical Principles of Organic Reactivity*; John Wiley & Sons: New York, 1995.
- (44) Ingold, K. U.; Robert, B. P. *Free-Radical Substitution Reactions*; Wiley-Interscience: New York, 1971.
- (45) Evans, M. G.; Polanyi, M. *Trans. Faraday Soc.* **1938**, *34*, 11.
- (46) Marcus, R. A. *J. Chem. Phys.* **1956**, *24*, 966.
- (47) Marcus, R. A. *J. Phys. Chem.* **1968**, *72*, 891.
- (48) Jing, L.; Guler, L. P.; Nash, J. J.; Kenttämaa, H. I. *J. Am. Soc. Mass Spectrom.* **2004**, *15*, 913.
- (49) *CRC Handbook of Chemistry and Physics*, 78th ed.; Lide, D. R., Ed.; CRC Press: Boca Raton, 1997.
- (50) Heberger, K.; Lopata, A. *J. Org. Chem.* **1998**, *63*, 8646.
- (51) (a) Donahue, N. M.; Clarke, J. S.; Anderson, J. G. *J. Phys. Chem. A* **1998**, *102*, 3923. (b) Donahue, N. M. *J. Phys. Chem. A* **2001**, *105*, 1489. (c) Clarke, J. S.; Kroll, J. H.; Donahue, N. M.; Anderson, J. G. *J. Phys. Chem. A* **1998**, *102*, 9847. (d) Clarke, J. S.; Rypkema, H. A.; Kroll, J. H.; Donahue, N. M.; Anderson, J. G. *J. Phys. Chem. A* **2000**, *104*, 4458.
- (52) (a) Shaik, S. *J. Mol. Liq.* **1994**, *61*, 49. (b) Shaik, S.; Shurki, A. *Angew. Chem., Int. Ed.* **1999**, *38*, 586.
- (53) In the ionic avoided curve crossing model, it is the vertical IE of the X–H bond of the hydrogen atom donor that is associated with the hypothetical ionic excited state of the reactants. Since it is extremely difficult, if not impossible, to determine the IE for a specific chemical bond in a polyatomic molecule (e.g., a hydrogen atom donor), the IE of the molecule is used as an approximation for the energy of the hypothetical ionic excited state.
- (54) (a) In *Free Radicals*; Kochi, J. K., Ed.; John Wiley & Sons: New York, 1973; Vol. 1. (b) Fossey, J.; Lefort, D.; Sorba, J. In *Free Radicals in Organic Chemistry*; John Wiley & Sons: New York, 1995. (c) Tedder, J. M. *Angew. Chem., Int. Ed., Engl.* **1982**, *21*, 401.
- (55) Vorob'ev, A. S.; Furler, I. I.; Sultanov, A. S.; Khvostenko, V. I.; Leplyanin, G. V.; Derzhinskii, A. R.; Tolstikov, G. A. *Bull. Acad. Sci. USSR, Div. Chem. Sci.* **1989**, 1388.
- (56) Ohno, K.; Imai, K.; Harada, Y. *J. Am. Chem. Soc.* **1985**, *107*, 8078.
- (57) Similar products have also been observed for the reaction of tetrahydrofuran with the related σ,σ,σ -triradical, 3,4,5-tridehydropyridinium cation: Jankiewicz, B. J.; Reece, J. N.; Vinueza, N. R.; Nash, J. J.; Kenttämaa, H. I. *Angew. Chem., Int. Ed.* **2008**, *47*, 9860.